ELSEVIER

International Journal of Mass Spectrometry 192 (1999) 111–123

International Journal of Mass Spectrometry

An experimental and computational study of the double ionization of CH_3Cl, CH_2Cl_2, and $CHCl_3$ molecules to singlet and triplet electronic states of their dications

R.P. Grant[a], F.M. Harris[a,*], D.E. Parry[b]

[a]*Mass Spectrometry Research Unit,* [b]*Department of Chemistry, University of Wales Swansea, Singleton Park, Swansea SA2 8PP, UK*

Received 11 November 1998; accepted 8 April 1999

Abstract

Experimental and computational methods were applied to study the double ionization of the molecules CH_3Cl, CH_2Cl_2, and $CHCl_3$. Double-charge-transfer spectroscopy was applied to measure the double-ionization energies of the molecules. The translational energies of the negative ions generated when fast-moving singly charged positive projectile ions acquire two electrons in collisions with the molecules provides information on the states of the dications populated. The use of H^+, OH^+, and F^+ projectile ions allowed transitions to singlet and triplet electronic states of the dications to be studied. Double-ionization energies to those states were calculated using the second order algebraic diagrammatic construction Green's function method. The calculated and measured values for CH_3Cl were found to be in good agreement. The computed data predicted that the density of states for $CH_2Cl_2^{2+}$ and $CHCl_3^{2+}$ were much higher than for CH_3Cl^{2+}. On grouping the calculated double-ionization energies to close-lying states together, however, good agreement with the measured values was evident. The combined experimental and computational study reported here thus provides a detailed understanding of the double ionization of the three molecules to singlet and triplet electronic states of their dications. (Int J Mass Spectrom 192 (1999) 111–123) © 1999 Elsevier Science B.V.

Keywords: Ion-molecule collisions; Double-ionization energies; DCT spectroscopy; Green's function calculations

1. Introduction

An experimental technique where the double-ionization energies of molecules to electronic states of their dications can be measured is double-charge-transfer (DCT) spectroscopy. It is based on double-electron-capture (DEC) reactions that can be represented by

$$A^+ + M \rightarrow A^- + M^{2+} \quad (1)$$

where a fast-moving singly charged positive ion A^+ acquires two electrons from the molecule M under investigation which may be regarded as at rest. The reactions are endoergic, so the translational energy of A^- is lower than that of A^+. The difference in the translational energies depends on the electronic state of M^{2+} that is populated.

DCT spectroscopy is of considerable value in the study of the double ionization of molecules because it

* Corresponding author.

PII S1387-3806(99)00087-1

does not rely on the M^{2+} ion generated being stable; information on the energetics of the reaction is basically obtained from the translational energy of A^- if the translational energy of A^+ is constant. In addition, double ionization to both singlet and triplet states of the dications can be obtained because the DEC reactions obey the Wigner spin-conservation rule [1]. Thus, the choice of projectile ion will determine the multiplicity of the states of M^{2+} populated [2]. If the molecule under investigation has a singlet ground state, then singlet states of its dication are populated when using H^+ as the projectile ion, and triplet states are populated when using OH^+ and F^+ projectile ions. Thus, a thorough investigation of the double ionization of a molecule to both singlet and triplet states of the dication is possible using those three projectile ions.

Early studies [3,4] of chloromethane molecules carried out in this laboratory used the OH^+ projectile ion, so double ionization to triplet states were investigated. Since that time, a spectrometer capable of much higher translational-energy resolving power has been developed [5] for DCT spectroscopy. This has been used to study, for example, the double ionization of CCl_4 [6]; considerably more peaks were observed in the spectra than were evident in the previous study [3]. Further, the H^+ projectile ion was also used so that double-ionization energies to singlet states of CCl_4^{2+} were measured in addition to those to triplet states. A computational study of the double ionization of CCl_4 formed part of this more recent investigation. This proved of considerable value, since the calculated results, when compared with the measured values, allowed the electronic transitions giving rise to the spectral peaks to be identified.

In the present article, results are reported of a combined computational and experimental study of the double ionization of CH_3Cl, CH_2Cl_2, and $CHCl_3$. The research had three main objectives.

(1) Using the high-resolution spectrometer, studies of these molecules were carried out using OH^+ and F^+ projectile ions in order to obtain more detailed information about the triplet-state profiles of the dications.

(2) The H^+ projectile ion was used so that double-ionization energies to singlet states of the dications would be determined for the first time.

(3) In the study of the double ionization of CCl_4 [6], a semiempirical form [7] of the MSXα computational method [8] was used. A considerably more sophisticated method, based on the second order algebraic diagrammatic construction [ADC(2)] ab initio method, was used in the present study which overcame some of the shortcomings of the multiple scattering Xα (MSXα) method. By comparing the predicted double-ionization energies with those measured, it was anticipated that the electronic transitions giving rise to the DCT spectral peaks would be identified, thus giving a detailed understanding of the double ionization of the three molecules.

2. Experimental

The DCT spectrometer used is based on a commercial double-focusing mass spectrometer, a Finnigan 8230 (Finnigan MAT, Bremen, Germany), which has been adapted [5] for DCT spectroscopy. It has reversed geometry, i.e. the magnet is situated between the source and the electric sector. The projectile ions H^+ and OH^+ were generated by electron ionization of water, and F^+ by electron ionization of carbon tetrafluoride. They were accelerated to 3 keV translational energy, and mass selected using the magnet. The molecules under investigation were contained in a collision-gas cell located close to the intermediate focal point between the magnet and the electric sector. The projectile ions passed through the cell, and a fraction of them underwent DEC reaction (1). The negative ions generated were transmitted to the detector by reversing the polarities of the voltages applied to the electric sector's plates. A spectrum was obtained by scanning the voltages and recording the negative-ion currents using a Keithley data-acquisition system. The signal-to-noise ratio was improved by adding together numerous scans taken over the same voltage-scan range.

If E_p represents the translational energy of A^+ and

E_n(M) that of the A^- ion generated in the DEC reaction with a molecule M, then

$$E_p - E_n(\mathrm{M}) = \mathrm{DIE}(\mathrm{M}) - E(\mathrm{A}^+ \rightarrow \mathrm{A}^-) \quad (2)$$

where DIE(M) represents the double-ionization energy of M and $E(A^+ \rightarrow A^-)$ is the energy released in the charge inversion from A^+ to A^-. The relationship between the electric-sector voltages and the translational energy of the transmitted ions is known, so the spectrum obtained is that of negative-ion current as a function of E_n(M). Peaks in the spectrum will appear as different electronic states of M^{2+} are populated. To derive double-ionization energies from the spectrum recorded, it is necessary to convert the E_n scale into a double-ionization energy scale. This is done in a calibration procedure using a DCT spectrum obtained with an atom such as xenon for which DIE(Xe) values are known.

Then,

$$E_p - E_n(\mathrm{Xe}) = \mathrm{DIE}(\mathrm{Xe}) - E(\mathrm{A}^+ \rightarrow \mathrm{A}^-) \quad (3)$$

where E_n(Xe) is the peak position for a specific electronic transition to a state in Xe^{2+} having a known DIE(Xe). In this way, the negative-ion translational-energy scale is converted to a double-ionization-energy scale.

3. Theoretical

The double-ionization energies observed are the vertical energy differences between the initial neutral molecule ground state and those final dication states, having the same geometric structure as the initial state, which are populated in the fast DCT reactions. A straightforward approach to their prediction would be to perform separate calculations of the energies of the initial state and of each final state of interest, but for vertical transitions a much more efficient procedure is to calculate the energy differences directly using a propagator method. Information required for the description of the double-ionization process is contained in the *pp* propagator, the equal-time two-particle Green's function for the *N*-electron neutral molecule with both particles (electrons) created simultaneously at time t', and destroyed simultaneously at time t''. Matrix elements of the Fourier transform of the *pp* propagator for $t'' < t'$ exhibit a pole wherever the energy variable in the transform coincides with a DIE. The ADC method [9] is based on the observation that an unitary transformation converts a closure sum in the propagator over the dication eigenstates m into sums over the "main" two-hole ($2h$) and "satellite" [$3h1p$, $4h2p$, etc., which are $2h$ configurations with various degrees of particle–hole shakeup (ph)] configurations that may be constructed from the self-consistent field (SCF) molecular orbitals, so that the diagonal matrix with energy-difference elements $E_m^{N-2} - E_0^N$ transforms into a matrix **K** in the configuration basis. **K** may be constructed explicitly in terms of the energies of, and two-electron integrals over, the SCF molecular orbitals [9] and its diagonalization will yield the desired DIEs. To the second or third order in perturbation theory, the only nonzero off-diagonal matrix elements of **K** are between $2h$ and $3h1p$ configurations, so that the DIEs are eigenvalues of a **K** matrix of dimension equal to the number of those configurations [9] (in practice, space and spin symmetries are exploited so that each symmetry block of **K** is diagonalized separately). Strictly, in the ADC(2) approximation terms of up to the second order in two-electron interaction integrals are included in the $2h$–$2h$ matrix elements, up to first order in the $2h$–$3h1p$ matrix elements, and the $3h1p$–$3h1p$ matrix elements are of order zero, but two further levels of approximation are employed in this work. For CH_3Cl and CH_2Cl_2 all first order terms are also included in the $3h1p$–$3h1p$ matrix elements in the "enhanced" ADC(2) approximation which has had widespread application [10–14]. For $CHCl_3$ only the diagonal $3h1p$–$3h1p$ matrix elements are augmented with such first-order terms in a "diagonal" approximation [15–17], which introduces considerable computational economy into the diagonalization of each **K** for this larger molecule at the expense of a slight but acceptable degradation in quality of the predicted DIEs [16,17].

A polarized double-zeta (DZP) basis set was employed in the ab initio calculations which were carried out with the GAUSSIAN94 [18] program package coupled with in-house FORTRAN code for the

Table 1
Hartree-Fock molecular orbital energies for CH_3Cl, CH_2Cl_2 and $CHCl_3$, calculated as described in the text

CH_3Cl		CH_2Cl_2		$CHCl_3$	
M.O.	ϵ (eV)	M.O.	ϵ (eV)	M.O.	ϵ (eV)
		$6a_1$	−32.46		
		$5b_2$	−29.77	$6a_1$	−33.95
		$7a_1$	−24.48	$6e$	−30.38
		$2b_1$	−18.56	$7a_1$	−23.85
		$8a_1$	−16.74	$8a_1$	−18.64
$5a_1$	−30.60	$6b_2$	−15.82	$7e$	−17.07
$6a_1$	−24.73	$2a_2$	−12.75	$8e$	−13.65
$2e$	−16.72	$9a_1$	−12.72	$9e$	−12.67
$7a_1$	−14.69	$3b_1$	−12.08	$9a_1$	−12.63
$3e$	−11.67	$7b_2$	−12.04	$2a_2$	−12.19
$8a_1$	5.37	$10a_1$	4.59	$10a_1$	3.84
$9a_1$	7.54	$8b_2$	5.62	$10e$	5.43
$4e$	8.59	$11a_1$	7.67	$11a_1$	8.37
$10a_1$	11.73	$4b_1$	9.45	$11e$	11.16
$5e$	12.06	$12a_1$	11.00	$12a_1$	11.53
		$9b_2$	11.23		
		$5b_1$	11.38		

ADC(2) calculations [14]. The experimentally determined neutral molecule geometries were: CH_3Cl (C_{3v}), R(C–H) = 109.59 pm, R(C–Cl) = 178.123 pm, ∠HCCl = 108.0° [19]; CH_2Cl_2 (C_{2v}), R(C–H) = 106.8 pm, R(C–Cl) = 177.24 pm, ∠HCH = 112.0°, ∠ClCCl = 111.8° [20]; $CHCl_3$ (C_{3v}), R(C–H) = 107.3 pm, R(C–Cl) = 176.2 pm, ∠HCCl = 108.0° [21]. For each molecule, the Hartree-Fock molecular orbitals were first calculated and the energies of, and two-electron integrals over, them (see Table 1) were then input to the ADC(2) calculations. Tables 2–7 contains both the theoretical and experimental data for a particular molecule and spin symmetry. The first column in each gives the symmetries of the transitions, which are also those of the final dication states because each neutral molecule has a $^1A_1$ ground state; the second column lists the weights of main $2h$ configurations (satellite states, arbitrarily defined as having less than 20% main character, are not expected to be populated significantly in DCT collisions [22]); leading configurations for the transitions are given in the third column. Many of the ADC(2) predictions of DIEs in the fourth columns are too closely spaced in energy to be distinguished experimentally and therefore those of main transitions have to be grouped so that the mean DIE of the group is then considered. It is now established that while relative energy separations of ADC(2) DIEs are accurate, all predicted DIEs for a given molecule require the addition of an uniform energy shift to achieve a sensible alignment with the experimental values [10–14]; the fifth columns list those shifted values, grouped where appropriate. For brevity, only those predicted DIEs in and just above the energy range accessed experimentally are given, while details of predicted satellites are only given explicitly, italicized, within that range.

4. Results

4.1. Calibration spectra

A typical H^+/Xe spectrum is shown in Fig. 1. The dominant peak B is due to the populating of the $^1D_2$ state of Xe^{2+} for which DIE(Xe) = 35.447 eV [23]. Its position provides the E_n(Xe) value required in Eq. (3). It has been shown [24] that spin is not strictly conserved in DEC reactions with a large atom such as

Table 2
Theoretical and experimental results for double ionizations of CH_3Cl to singlet states of CH_3Cl^{2+}. Main double-ionization energies predicted in the ADC(2) approximation have been grouped where appropriate before application of a uniform shift of +1.2 eV. Satellite states, listed in italics, are not expected to be populated significantly in DCT spectroscopy

Term	Main %	Leading configurations	DIE (eV)	Group DIE (eV + 1.2)	DCT (eV)	Peak[a]
^1E	87	70% $3e^{-2}$	30.76	32.2	32.3 ± 0.2	1
$^1A_1$	88	61% $3e^{-2}$	31.32			
$^1A_2$	88	88% $2e^{-1}3e^{-1}$	32.60	33.8	33.6 ± 0.3	2
^1E	86	81% $7a_1^{-1}3e^{-1}$	34.02	35.6	35.4 ± 0.3	3
^1E	83	65% $2e^{-1}3e^{-1}$	34.78			
$^1A_1$	83	54% $2e^{-1}3e^{-1}$, 19% $3e^{-2}$	35.65	36.9	36.5 ± 0.3	4
^1E	86	77% $2e^{-1}7a_1^{-1}$	37.44	38.7	38.5 ± 0.3	5
$^1A_1$	85	75% $7a_1^{-2}$	37.50			
^1E	76	62% $2e^{-2}$	40.05	41.3	40.4 ± 0.3	6
^1E	*3*	*33% $3e^{-3}8a_1$, 24% $2e^{-1}3e^{-2}8a_1$*	*40.80*			
^1E	76	48% $6a_1^{-1}3e^{-1}$	41.48	42.8	42.2 ± 0.3	7
$^1A_1$	78	67% $2e^{-2}$	41.78			
		7 satellites				
$^1A_1$	60	56% $6a_1^{-1}7a_1^{-1}$	45.81	46.8		

[a] See Fig. 3.

Table 3
Theoretical and experimental results for double ionizations of CH_3Cl to triplet states of CH_3Cl^{2+}. Main double-ionization energies predicted in the ADC(2) approximation have been grouped where appropriate before application of a uniform shift of +1.2 eV. Satellite states, listed in italics, are not expected to be populated significantly in DCT spectroscopy

Term	Main %	Leading configurations	DIE (eV)	Group DIE (eV + 1.2)	DCT (eV)	Peak[a]
$^3A_2$	86	80% $3e^{-2}$	29.81	31.0	31.5 ± 0.2	A
^3E	89	88% $2e^{-1}3e^{-1}$	32.73	34.0	34.1 ± 0.2	B
$^3A_1$	89	89% $2e^{-1}3e^{-1}$	32.82			
^3E	86	84% $7a_1^{-1}3e^{-1}$	32.89			
$^3A_2$	84	78% $2e^{-1}3e^{-1}$	33.67	34.9	35.5 ± 0.3	C
^3E	85	83% $2e^{-1}7a_1^{-1}$	36.91	38.1 } 39.0	39.0 ± 0.3	D
$^3A_2$	78	77% $2e^{-2}$	38.75	40.0 }		
^3E	*16*	*28% $3e^{-3}8a_1$, 16% $6a_1^{-1}3e^{-1}$*	*39.65*			
^3E	62	61% $6a_1^{-1}3e^{-1}$	40.02	41.2	41.0 ± 0.3	E
		8 satellites				
$^3A_1$	77	76% $6a_1^{-1}2e^{-1}$	43.26	44.5		

[a] See Fig. 4.

Table 4
Theoretical and experimental results for double ionizations of CH_2Cl_2 to singlet states of $CH_2Cl_2^{2+}$. Main double-ionization energies predicted in the ADC(2) approximation have been grouped where appropriate before application of a uniform shift of +1.3 eV. Satellite states, listed in italics, are not expected to be populated significantly in DCT spectroscopy

Term	Main %	Leading configurations	DIE (eV)	Group DIE (eV + 1.3)	DCT (eV)	Peak[a]
$^1A_1$	90	56% $3b_1^{-2}$, 32% $2a_2^{-2}$	27.80	29.3	29.3 ± 0.2	1
$^1A_2$	90	26% $3b_1^{-1}7b_2^{-1}$, 29% $2a_2^{-1}9a_1^{-1}$	28.05			
$^1B_1$	90	45% $9a_1^{-1}3b_1^{-1}$, 41% $2a_2^{-1}7b_2^{-1}$	28.21			
$^1A_1$	90	51% $7b_2^{-2}$, 31% $9a_1^{-2}$	28.50	29.8	30.0 ± 0.3	2
$^1B_2$	87	56% $9a_1^{-1}7b_2^{-1}$, 16% $8a_1^{-1}7b_2^{-1}$	31.00	32.4	33.0 ± 0.5	3
$^1A_2$	87	32% $2a_2^{-1}9a_1^{-1}$, 22% $6b_2^{-1}3b_1^{-1}$	31.06			
$^1A_1$	87	31% $9a_1^{-2}$, 20% $7b_2^{-2}$, 17% $6b_2^{-1}7b_2^{-1}$	31.24			
$^1B_1$	87	26% $2a_2^{-1}7b_2^{-1}$, 25% $9a_1^{-1}3b_1^{-1}$	31.25			
$^1B_2$	82	60% $2a_2^{-1}3b_1^{-1}$, 20% $2b_1^{-1}2a_2^{-1}$	32.04	34.0	33.9 ± 0.2	4
$^1A_1$	83	33% $2a_2^{-2}$, 21% $3b_1^{-2}$, 18% $2b_1^{-1}3b_1^{-1}$	32.42			
$^1A_2$	84	36% $2b_1^{-1}7b_2^{-1}$, 22% $6b_2^{-1}3b_1^{-1}$	33.01			
$^1B_1$	83	22% $6b_2^{-1}2a_2^{-1}$, 21% $2b_1^{-1}9a_1^{-1}$, 20% $8a_1^{-1}3b_1^{-1}$	33.18			
$^1A_1$	83	54% $6b_2^{-1}7b_2^{-1}$	34.15	35.6	35.4 ± 0.2	5
$^1A_2$	81	34% $6b_2^{-1}3b_1^{-1}$, 22% $2b_1^{-1}7b_2^{-1}$	34.45			
$^1B_2$	80	47% $6b_2^{-1}9a_1^{-1}$, 15% $9a_1^{-1}7b_1^{-1}$	35.03	36.7	36.9 ± 0.3	6
$^1B_1$	81	40% $6b_2^{-1}2a_2^{-1}$, 28% $8a_1^{-1}3b_1^{-1}$	35.20			
$^1A_1$	80	44% $8a_1^{-1}9a_1^{-1}$	35.21			
$^1B_2$	81	49% $8a_1^{-1}7b_2^{-1}$, *14% $6b_2^{-1}9a_1^{-1}$*	35.58			
$^1A_2$	79	41% $8a_1^{-1}2a_2^{-1}$, 22% $2b_1^{-1}7b_2^{-1}$	35.62			
$^1B_1$	79	53% $2b_1^{-1}9a_1^{-1}$	35.62			
$^1A_1$	78	43% $2b_1^{-1}3b_1^{-1}$	36.33	37.6	37.9 ± 0.3	7
$^1B_2$	77	45% $2b_1^{-1}2a_2^{-1}$, 15% $2a_2^{-1}3b_1^{-1}$	36.36			
$^1A_1$	82	53% $6b_2^{-2}$	37.13	38.4	39.1 ± 0.2	8
$^1B_2$	*2*	*51% $3b_1^{-2}7b_2^{-1}10a_1$*	*37.91*			
$^1A_2$	*4*	*60% $2a_2^{-1}3b_1^{-2}10a_1$*	*37.92*			
$^1A_1$	*2*	*50% $9a_1^{-1}3b_1^{-2}10a_1$*	*38.13*			
$^1B_1$	*1*	*42% $3b_1^{-1}7b_2^{-2}10a_1$, 23% $9a_1^{-2}3b_1^{-1}10a_1$*	*38.24*			
$^1B_2$	79	50% $8b_1^{-1}6b_2^{-1}$, 15% $7a_1^{-1}7b_2^{-1}$	38.36	39.9	39.9 ± 0.2	9
$^1A_1$	*0*	*53% $2a_2^{-1}3b_1^{-1}7b_2^{-1}10a_1$*	*38.45*			
$^1B_1$	12	28% $2a_2^{-2}3b_1^{-1}10a_1$, 27% $2a_2^{-1}3b_1^{-2}8b_2$	38.46			
$^1B_2$	*0*	*45% $2a_2^{-1}9a_1^{-1}3b_1^{-1}10a_1$*	*38.58*			
$^1A_2$	37	30% $9a_2^{-1}3b_1^{-1}7b_2^{-1}10a_1$, 27% $2b_1^{-1}6b_2^{-1}$	38.58			
$^1A_2$	37	27% $2b_1^{-1}6b_2^{-1}$, 21% $9a_1^{-1}3b_1^{-1}7b_2^{-1}10a_1$	38.67			
$^1A_1$	*2*	*41% $3b_1^{-2}7b_2^{-1}8b_2$*	*38.91*			
$^1B_1$	47	22% $7a_1^{-1}$, 19% $2b_1^{-1}8a_1^{-1}$	38.97			
		4 satellites				
$^1A_1$	75	53% $8a_1^{-2}$	39.37	40.7		

[a] See Fig. 5.

Xe, and the peak A is due to the populating of triplet states. Peak C, on the other hand, is due to the populating of the $^1S_0$ state, the double-ionization energy to which 37.963 eV [23].

When OH^+ and F^+ undergo DEC reactions with xenon, two peaks are observed (see, e.g. Fig. 2). The peak marked 1 is due to the populating of the $^3P_2$ of Xe^{2+} [DIE(Xe) = 33.327 eV [23]) and peak 2 is due

Table 5
Theoretical and experimental results for double ionizations of CH_2Cl_2 to triplet states of $CH_2Cl_2^{2+}$. Main double-ionization energies predicted in the ADC(2) approximation have been grouped where appropriate before application of a uniform shift of +1.3 eV. Satellite states, listed in italics, are not expected to be populated significantly in DCT spectroscopy

Term	Main %	Leading configurations	DIE (eV)	Group DIE (eV + 1.3)	DCT (eV)	Peak[a]
$^3B_2$	90	89% $2a_2^{-1}3b_1^{-1}$	27.86	29.3	29.6 ± 0.2	A
$^3A_2$	89	62% $3b_1^{-1}7b_2^{-1}$, 25% $2a_2^{-1}9a_1^{-1}$	27.98			
$^3B_1$	90	45% $9a_1^{-1}3b_1^{-1}$, 41% $2a_2^{-1}7b_2^{-1}$	28.11			
$^3B_2$	89	84% $9a_1^{-1}7b_2^{-1}$	28.42	29.7	30.3 ± 0.2	B
$^3B_1$	84	36% $2a_2^{-1}7b_2^{-1}$, 35% $9a_1^{-1}3b_1^{-1}$	30.49	31.8	31.6 ± 0.2	C
$^3A_2$	85	49% $2a_2^{-1}9a_1^{-1}$, 19% $3b_1^{-1}7b_2^{-1}$	30.55			
$^3A_1$	88	62% $6b_2^{-1}7b_2^{-1}$, 26% $8a_1^{-1}9a_1^{-1}$	32.10	33.7	33.7 ± 0.3	D
$^3B_2$	88	51% $8a_1^{-1}7b_2^{-1}$, 36% $6b_2^{-1}9a_1^{-1}$	32.28			
$^3A_2$	84	54% $6b_2^{-1}3b_1^{-1}$, 14% $8a_1^{-1}2a_2^{-1}$	32.59			
$^3B_1$	84	36% $6b_2^{-1}2a_2^{-1}$, 34% $8a_1^{-1}3b_1^{-1}$	32.72			
$^3B_2$	84	45% $6b_2^{-1}9a_1^{-1}$, 32% $8a_1^{-1}7b_1^{-1}$	33.57	35.1	34.6 ± 0.3	E
$^3A_2$	82	38% $2b_1^{-1}7b_2^{-1}$, 25% $8a_1^{-1}2a_2^{-1}$, 15% $6b_2^{-1}3b_1^{-1}$	33.81			
$^3A_1$	83	82% $2b_1^{-1}3b_1^{-1}$	33.90			
$^3B_1$	79	38% $8a_1^{-1}3b_1^{-1}$, 36% $6b_2^{-1}2a_2^{-1}$	34.01			
$^3B_2$	82	82% $2b_1^{-1}2a_2^{-1}$	34.33	35.9	35.8 ± 0.3	F
$^3A_1$	78	56% $8a_1^{-1}9a_1^{-1}$, 21% $6b_2^{-1}7b_2^{-1}$	34.43			
$^3A_2$	79	36% $8a_1^{-1}2a_2^{-1}$, 36% $2b_1^{-1}7b_2^{-1}$	34.54			
$^3B_1$	80	73% $2b_1^{-1}9a_1^{-1}$	34.92			
$^3B_2$	*0*	*48% $3b_1^{-2}7b_2^{-1}10a_1$*	*36.62*			
$^3A_1$	*0*	*39% $9a_1^{-1}3b_1^{-2}10a_1$*	*36.80*			
$^3B_2$	81	75% $8a_1^{-1}6b_2^{-1}$	36.86	38.2	37.8 ± 0.3	G
$^3B_1$	*2*	*33% $3b_1^{-1}7b_2^{-2}10a_1$, 24% $9a_1^{-2}3b_1^{-1}10a_1$*	*37.21*			
$^3A_2$	*1*	*35% $9a_1^{-1}3b_1^{-1}7b_2^{-1}10a_1$*	*37.40*			
$^3A_2$	*3*	*63% $2a_2^{-1}3b_1^{-2}10a_1$*	*37.62*			
$^3B_2$	*1*	*29% $2a_2^{-1}9a_1^{-1}3b_1^{-1}10a_1$*	*37.69*			
$^3A_1$	*1*	*31% $2a_2^{-1}3b_1^{-1}7b_2^{-1}10a_1$*	*37.70*			
$^3A_2$	*1*	*34% $9a_1^{-1}3b_1^{-1}7b_2^{-1}10a_1$*	*38.03*			
$^3B_1$	*15*	*20% $2a_2^{-2}3b_1^{-1}10a_1$, 14% $7a_1^{-1}3b_1^{-1}$*	*38.24*			
$^3A_2$	48	44% $2b_1^{-1}6b_2^{-1}$	38.25	39.6	38.7 ± 0.3	H
$^3A_1$	*2*	*11% $2a_2^{-2}9a_1^{-1}10a_1$, 10% $2a_2^{-1}3b_1^{-1}7b_2^{-1}10a_1$*	*38.25*			
$^3A_1$	*0*	*61% $2a_2^{-1}3b_1^{-1}7b_2^{-1}10a_1$*	*38.37*			
$^3B_2$	*9*	*No dominant configuration*	*38.40*			
$^3B_1$	*1*	*No dominant configuration*	*38.41*			
$^3B_1$	*19*	*No dominant configuration*	*38.50*			
$^3A_2$	34	29% $2b_1^{-1}6b_2^{-1}$	38.51	39.9	39.5 ± 0.3	I
$^3B_2$	*6*	*19% $2a_2^{-1}9a_1^{-1}3b_1^{-1}10a_1$*	*38.62*			
$^3A_2$	*0*	*26% $9a_1^{-1}3b_1^{-1}7b_2^{-1}10a_1$*	*38.62*			
$^3A_1$	*0*	*22% $3b_1^{-2}7b_2^{-1}8b_2$*	*38.63*			
$^3B_2$	*4*	*33% $2a_2^{-1}9a_1^{-1}3b_1^{-1}10a_1$*	*38.72*			
$^3B_1$	33	24% $7a_1^{-1}3b_1^{-1}$	38.77			
$^3A_1$	*3*	*41% $9a_1^{-1}7b_2^{-2}10a_1$*	*38.82*			
$^3B_2$	*6*	*12% $9a_1^{-2}7b_2^{-1}10a_1$*	*38.83*			
$^3B_1$	*6*	*25% $9a_1^{-1}3b_1^{-1}7b_2^{-1}8b_2$*	*38.83*			
$^3B_2$	45	36% $7a_1^{-1}7b_2^{-1}$, 25% $9a_1^{-2}7b_2^{-1}10a_1$	39.02	41.4		
$^3B_1$	60	53% $2b_1^{-1}8a_1^{-1}$	39.11			
$^3A_2$	31	25% $7a_1^{-1}2a_2^{-1}$	39.11			
$^3A_2$	15	12% $7a_1^{-1}2a_2^{-1}$	39.19			
$^3B_1$	*0*	*19% $2a_2^{-1}3b_1^{-2}8b_2$, 16% $2b_1^{-1}3b_1^{-2}10a_1$*	*39.23*			
$^3B_1$	*1*	*25% $9a_1^{-1}3b_1^{-1}7b_2^{-1}8b_2$*	*39.25*			
$^3A_1$	60	53% $7a_1^{-1}9a_1^{-1}$	39.30			

[a] See Fig. 6.

Table 6
Theoretical and experimental results for double ionizations of $CHCl_3$ to singlet states of $CHCl_3^{2+}$. Main double-ionization energies predicted in the ADC(2) approximation have been grouped where appropriate before application of a uniform shift of +1.5 eV

Term	Main %	Leading configurations	DIE (eV)	Group DIE (eV + 1.5)	DCT (eV)	Peak[a]
$^1A_1$	88	65% $2a_2^{-2}$	27.76	29.7	29.9 ± 0.2	1
$^1A_2$	88	70% $9a_1^{-1}2a_2^{-1}$	27.98			
^1E	88	28% $9e^{-1}2a_2^{-1}$, 24% $9e^{-2}$	28.03			
$^1A_1$	87	69% $9a_1^{-2}$	28.49			
^1E	87	24% $9e^{-1}9a_1^{-1}$	28.65			
^1E	87	35% $9e^{-2}$, 29% $8e^{-1}9a_1^{-1}$	29.03	30.7	30.9 ± 0.2	2
$^1A_1$	87	47% $9e^{-2}$	29.28			
^1E	87	29% $8e^{-1}9e^{-1}$	29.39			
^1E	84	28% $8e^{-1}2a_2^{-1}$	31.09	32.9	32.5 ± 0.3	3
$^1A_2$	82	52% $8e^{-1}9e^{-1}$	31.13			
^1E	82	22% $8e^{-2}$	31.35			
$^1A_1$	80	52% $8e^{-1}9e^{-1}$	31.55			
^1E	81	15% $9e^{-1}9a_1^{-1}$, 12% $8e^{-1}9a_1^{-1}$	31.75			
$^1A_1$	82	28% $8e^{-2}$	32.48	34.3	34.1 ± 0.2	4
$^1A_2$	85	47% $7e^{-1}9e^{-1}$, 35% $8a_1^{-1}2a_2^{-1}$	32.75			
^1E	82	26% $7e^{-1}9a_1^{-1}$	33.15			
^1E	79	49% $7e^{-1}9e^{-1}$	33.67	35.3	35.1 ± 0.2	5
^1E	76	33% $7e^{-1}2a_2^{-1}$	34.00			
^1E	77	51% $7e^{-1}9e^{-1}$	34.40	36.0	35.6 ± 0.3	6
$^1A_1$	77	33% $7e^{-1}8e^{-1}$, 28% $8a_1^{-1}9a_1^{-1}$	34.64			
^1E	76	26% $7e^{-1}8e^{-1}$, 18% $8a_1^{-1}8e^{-1}$	35.03	36.8	36.7 ± 0.2	7
$^1A_2$	77	32% $7e^{-1}8e^{-1}$	35.03			
^1E	77	28% $8a_1^{-1}9e^{-1}$, 24% $7e^{-1}8e^{-1}$	35.23			
$^1A_1$	74	35% $8a_1^{-1}9a_1^{-1}$, 27% $7e^{-1}8e^{-1}$	35.45			
^1E	74	37% $8a_1^{-1}8e^{-1}$, 18% $8a_1^{-1}9e^{-1}$	35.65			
^1E	81	64% $7e^{-2}$	37.57	39.1	38.9 ± 0.3	8
$^1A_1$	79	53% $7e^{-2}$	38.23	40.0	40.3 ± 0.3	9
^1E	78	35% $7a_1^{-1}9e^{-1}$, 34% $8a_1^{-1}7e^{-1}$	38.56			
$^1A_2$	76	76% $7a_1^{-1}2a_2^{-1}$	38.64			
$^1A_1$	75	47% $7a_1^{-1}9a_1^{-1}$	39.51	41.2		
^1E	75	37% $8a_1^{-1}7e^{-1}$, 22% $7a_1^{-1}9e^{-1}$	39.55			
^1E	76	53% $7a_1^{-1}8e^{-1}$	39.83			
$^1A_1$	74	63% $8a_1^{-2}$	40.77	42.3		

[a] See Fig. 7.

to the populating of the $^3P_0$ and $^3P_1$ states which lie within 0.212 eV of one another and have a mean DIE(Xe) of 34.441 eV [23].

Spectra similar to those of Figs. 1 and 2 were recorded in the present investigation to provide the relevant E_n(Xe) values.

4.2. Double ionization of CH_3Cl

Thirty four H^+/CH_3Cl spectra were recorded. After each spectrum a H^+/Xe calibration spectrum was recorded, which allowed the translational-energy scale for H^- to be converted into a double-ionization

Table 7
Theoretical and experimental results for double ionizations of $CHCl_3$ to triplet states of $CHCl_3^{2+}$. Main double-ionization energies predicted in the ADC(2) approximation have been grouped, where appropriate, before application of a uniform shift of +1.5 eV

Term	Main %	Leading configurations	DIE (eV)	Group DIE (eV + 1.5)	DCT (eV)	Peak[a]
$^3A_2$	87	62% $9a_1^{-1}2a_2^{-1}$	27.70	29.2	29.5 ± 0.2	A
^3E	87	72% $9e^{-1}2a_1^{-1}$	27.74			
^3E	87	60% $9e^{-1}9a_1^{-1}$	28.16	29.9	30.3 ± 0.3	B
$^3A_2$	86	43% $9e^{-2}$	28.37			
^3E	87	54% $8e^{-1}2a_2^{-1}$, 25% $8e^{-1}9a_1^{-1}$	28.53			
^3E	86	38% $8e^{-1}9a_1^{-1}$, 33% $8e^{-1}9e^{-1}$	28.97	30.6	31.0 ± 0.3	C
$^3A_1$	87	84% $8e^{-1}9e^{-1}$	29.07			
$^3A_2$	85	65% $8e^{-1}9e^{-1}$	29.40			
^3E	78	39% $8e^{-1}9e^{-1}$	30.30	32.0	32.5 ± 0.3	D
$^3A_2$	81	63% $8e^{-2}$	30.68			
^3E	84	71% $7e^{-1}2a_1^{-1}$	32.16	33.7	33.9 ± 0.3	E
^3E	82	50% $7e^{-1}9a_1^{-1}$, 28% $7e^{-1}9e^{-1}$	32.61	34.4	34.5 ± 0.3	F
^3E	84	67% $7e^{-1}9e^{-1}$	32.72			
^3E	81	41% $7e^{-1}9e^{-1}$, 23% $7e^{-1}9a_1^{-1}$	33.06			
$^3A_2$	82	49% $8a_1^{-1}2a_2^{-1}$, 27% $7e^{-1}8e^{-1}$	33.08			
$^3A_1$	83	43% $7e^{-1}8e^{-1}$, 39% $8a_1^{-1}9a_1^{-1}$	33.30			
^3E	80	64% $8a_1^{-1}9e^{-1}$	33.59	35.3	35.3 ± 0.3	G
$^3A_2$	78	50% $7e^{-1}8e^{-1}$	33.82			
^3E	78	59% $7e^{-1}8e^{-1}$	33.96			
$^3A_1$	76	36% $8a_1^{-1}9a_1^{-1}$, 26% $7e^{-1}8e^{-1}$	34.14			
^3E	77	69% $8a_1^{-1}8e^{-1}$	34.76	36.3	36.3 ± 0.3	H
$^3A_2$	81	67% $7e^{-2}$	36.93	38.4	38.2 ± 0.3	I
$^3A_2$	76	62% $7a_1^{-1}2a_2^{-1}$	37.78	39.6	39.4 ± 0.3	J
^3E	79	40% $8a_1^{-1}7e^{-1}$, 38% $7a_1^{-1}9e^{-1}$	37.96			
$^3A_1$	78	76% $7a_1^{-1}9a_1^{-1}$	38.13			
^3E	75	38% $7a_1^{-1}9e^{-1}$, 36% $8a_1^{-1}7e^{-1}$	38.33			
^3E	77	75% $7a_1^{-1}8e^{-1}$ *12 satellites*	38.99	40.5		
^3E	26	22% $8e^{-1}9a_1^{-1}2a_2^{-1}10a_1$	42.15	43.7		

[a] See Fig. 8.

energy scale. A typical H^+/CH_3Cl spectrum is shown in Fig. 3. The double-ionization energies corresponding to the seven peaks from all the recorded spectra have been averaged, and the mean values, together with their standard deviations, are shown in the sixth column of Table 2. On comparing the calculated and measured values, it can be seen that good agreement is evident, which allows the spectral peaks to be identified with specific transitions to singlet states of CH_3Cl^{2+} in the double-ionization process.

The transitions to triplet states of CH_3Cl^{2+} were studied experimentally using the OH^+ and F^+ projectile ions. In all, 36 spectra were recorded, typical examples of which are shown in Fig. 4. The differences in the spectra arise because the DEC reaction (1) has a low probability outside of a "reaction window" of endoergicities. The existence of such a window was predicted in two theoretical studies [25,26] but neither gave the upper and lower limits. In a subsequent experimental study [27], it was con-

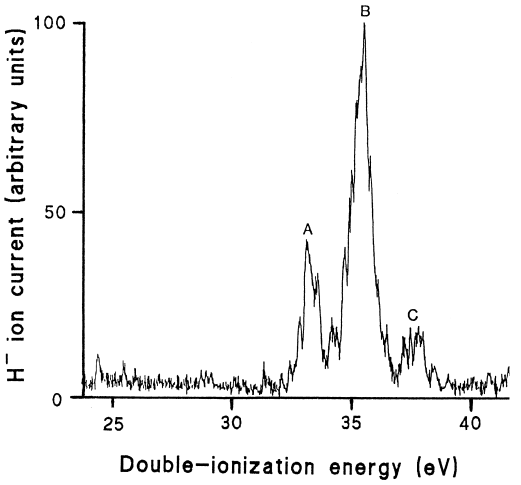

Fig. 1. A typical DCT spectrum recorded when H^+ ions underwent double-electron-capture reactions with xenon atoms.

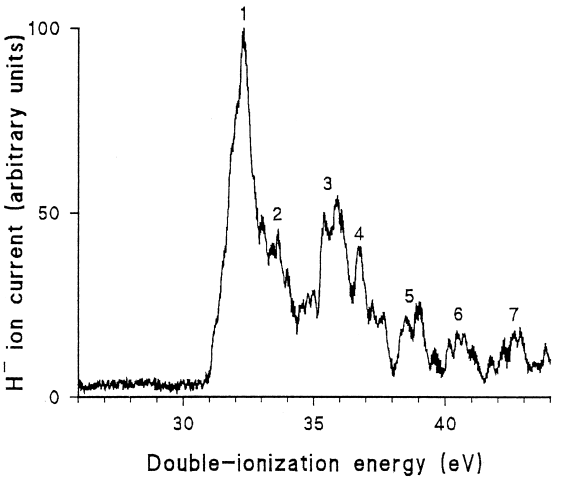

Fig. 3. A typical DCT spectrum recorded when H^+ ions underwent double-electron-capture reactions with CH_3Cl molecules.

cluded that for CH_3Br the window existed between 8 and 22 eV. It has since been found that those limits apply to numerous organic molecules [2]. Since the endoergicity is DIE(M) $-$ $E(A^+ \rightarrow A^-)$, it follows that higher DIE(M) values are more effectively investigated using larger values of $E(A^+ \rightarrow A^-)$. For OH^+, $E(OH^+ \rightarrow OH^-)$ is 14.8 eV although for F^+, $E(F^+ \rightarrow F^-)$ is 20.8 eV. It follows that the use of F^+ will probe higher-lying DIE(M) values more effectively. The average values of DIE(CH_3Cl) of the results from all the spectra are shown in Table 3 together with their standard deviations. Good agreement between the experimental and calculated DIE(CH_3Cl) values is evident.

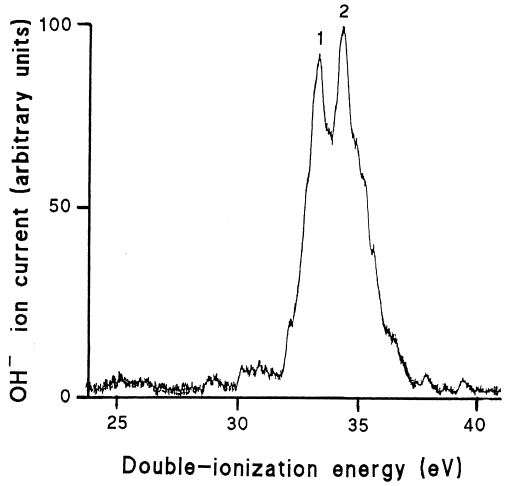

Fig. 2. A typical DCT spectrum recorded when OH^+ ions underwent double-electron-capture reactions with xenon atoms.

4.3. Double ionization of CH_2Cl_2 and $CHCl_3$

Typical DCT spectra obtained when studying these molecules are shown in Figs. 5–8, and the average DIEs, determined as outlined above, are shown in Tables 4–7. It can be seen that the density of states for $CH_2Cl_2^{2+}$ and $CHCl_3^{2+}$ is predicted from the computational study to be much higher than that for CH_3Cl^{2+}. However, as can be seen from Tables 4–7, logical groupings of the states are possible, which give average values in agreement with those determined from the spectral-peak positions.

5. Discussion

It is now established, from analyses of the DCT spectra of many molecules, that the energy of a doubly ionized state, created by the removal of two electrons from molecular spin-orbitals *a* and *b* of a neutral molecule, is to a good first approximation given by

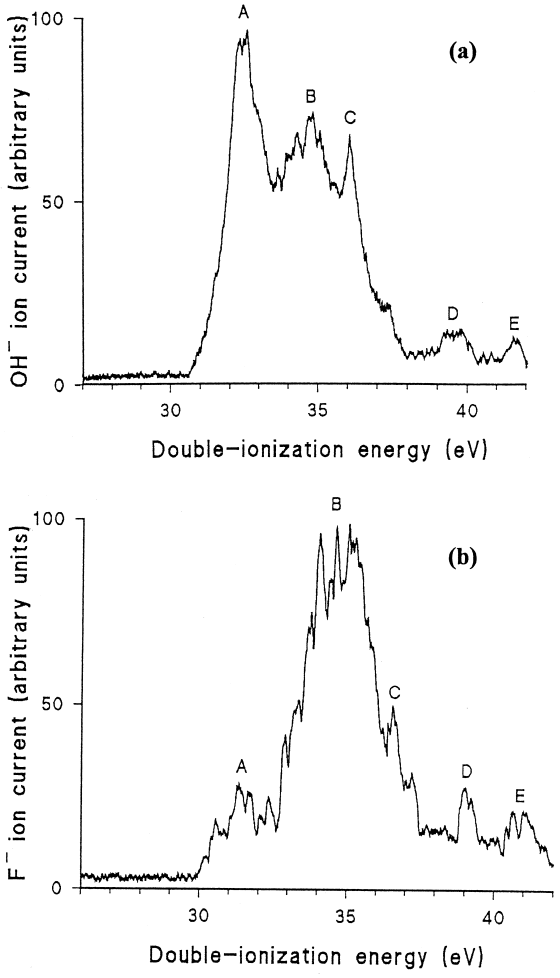

Fig. 4. Typical DCT spectra recorded when (a) OH^+ and (b) F^+ ions underwent double-electron-capture reactions with CH_3Cl molecules.

$$\mathrm{DIE}(a, b) \approx \mathrm{IE}(a) + \mathrm{IE}(b) + V_2 \quad (4)$$

where IE(a) is the single ionization energy associated with a and V_2 is a measure of the coulomb repulsion between any two valence holes created in that molecule, being in practice insensitive to the particular $2h$ configuration [7]. A semiempirical method [7] based on Eq. (4) can offer an effective preliminary analysis of DCT spectra of those molecules that have only one electronic term for each dication configuration. However, if the molecule has a non-Abelian structural symmetry group such as CH_3Cl and $CHCl_3$ studied in this article, then the ab initio method described above must be used to account for the various terms of different energies that may be associated with a configuration [14]. Nevertheless, Eq. (4) offers a straightforward means of relating DIEs to the molecular orbital energies of the neutral molecule if Koopmans' theorem is applied to it.

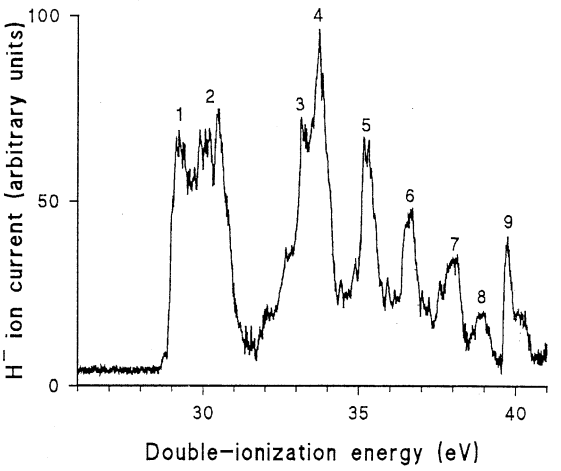

Fig. 5. A typical DCT spectrum recorded when H^+ ions underwent double-electron-capture reactions with CH_2Cl_2 molecules.

All three molecules studied here exhibit a large energy separation, ~15 eV, between the highest-occupied and lowest-unoccupied molecular orbitals of the neutral molecule (see Table 1). The implication of this is that, as the energy of any $3h1p$ satellite configuration will be greater than that of an associated $2h$ main configuration by the extra energy of creation of a ph pair, offset in part by the extra energy of attraction $-V_2$ for that electron–hole pair, satellite configurations will not contribute significantly to the lower energy states of the molecular dications. This is evident in Tables 2–7, where satellite dication states are found only at energies 10 eV or more above the ground dication state.

The CH_2Cl_2 molecule, which has the Abelian C_{2v} structural symmetry group, exhibits a large number of nondegenerate singlet and triplet dication states. In spite of the apparent complexity of the listings in Tables 4 and 5, most of the DIEs can be expressed in terms of the molecular orbital energies of the associ-

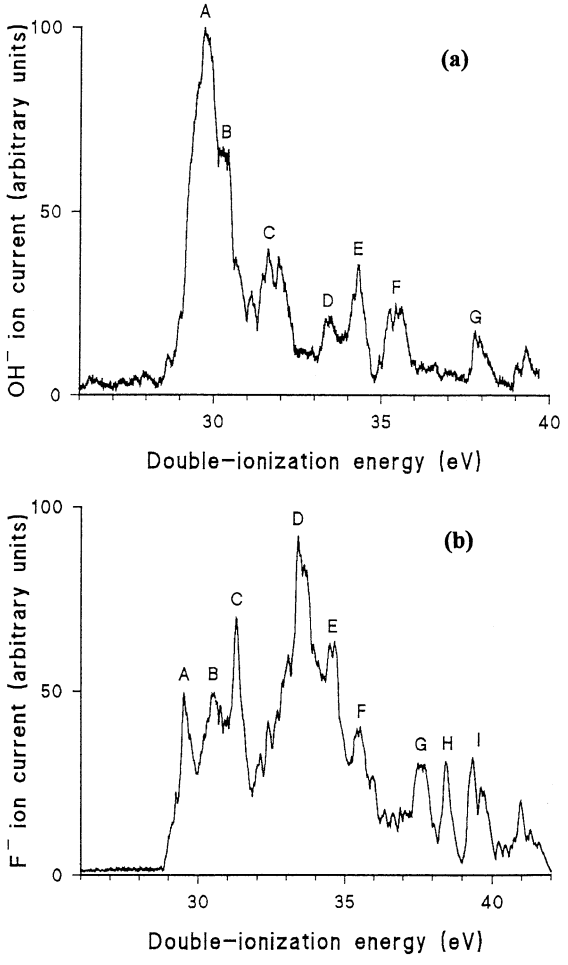

Fig. 6. Typical DCT spectra recorded when (a) OH^+ and (b) F^+ ions underwent double-electron-capture reactions with CH_2Cl_2 molecules.

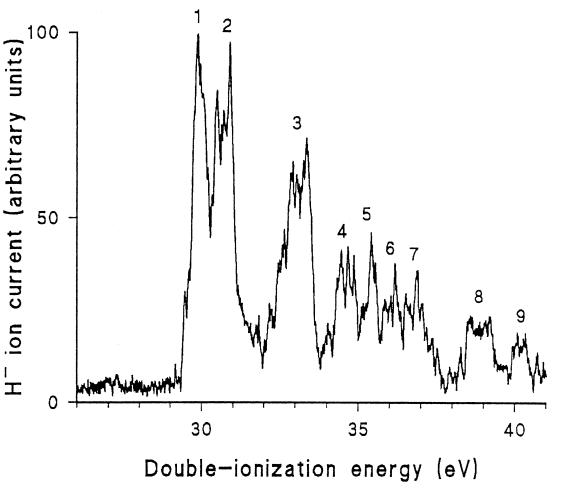

Fig. 7. A typical DCT spectrum recorded when H^+ ions underwent double-electron-capture reactions with $CHCl_3$ molecules.

ated dication configurations using Eq. (4), typical values of V_2 being 7 (singlets) and 4 eV (triplets); the lower range of V_2 values for triplets is expected because the two holes created in a symmetric triplet spin state will, on average, be further apart spatially than in the corresponding singlet configuration. Due to a relatively large number of higher-lying occupied molecular orbitals having similar energies (see Table 1), many configurations of CH_2Cl_2 are near degenerate and this has resulted both in strong configuration interaction in the dication states and in the energetic clustering of the dication states into groups which has favoured the matching of groups of states with the DCT peaks observed.

The value of V_2 is dominated by the coulomb repulsion of the two holes created in forming a dication configuration and therefore may be expected to decrease with increasing molecular volume. Application of Eq. (4) to the lowest state of CH_3Cl^{2+} in Tables 2 and 3 indicates that for this molecule V_2 has typical values of 8 (singlets) and 6 eV (triplets), consistent with the expected trend. However, main configurations of two *e* molecular orbitals may have A_1, A_2, and E associated terms, the energy separations that are not accounted for by Eq. (4). Similar considerations apply to $CHCl_3$, where V_2 values are typically 4 eV (singlets) and 3 eV (triplets).

The agreement between theoretical and experimental data in Tables 2–7 is most acceptable. Although the experimental resolution has required the grouping of theoretical values to enable a comparison, that has been possible in an obvious and transparent way. But the improvement in experimental resolution over that previously employed [4] has considerably enhanced our knowledge of the double-ionization processes in these molecules. The use of F^+ as a projectile ion in addition to OH^+ has enabled the experimental study of the transitions to higher-energy triplet dication

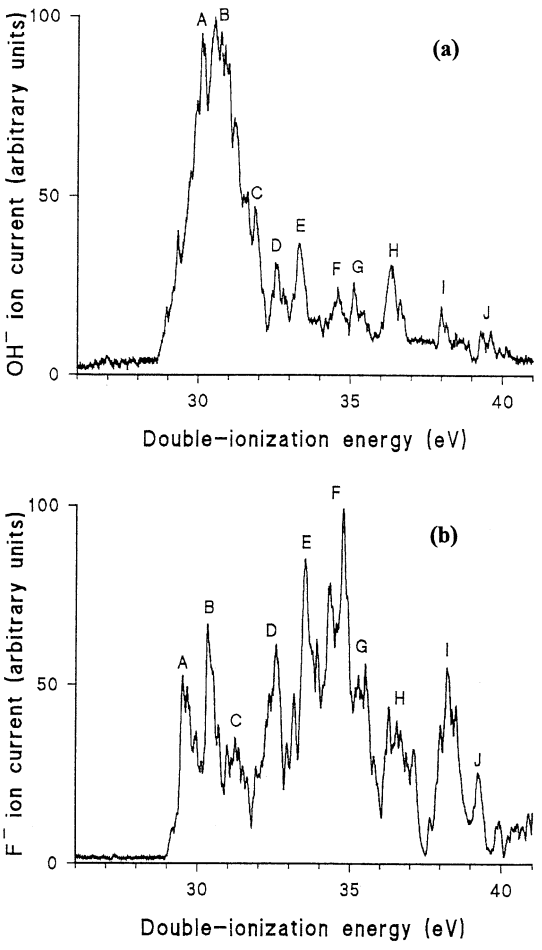

Fig. 8. Typical DCT spectra recorded when (a) OH^+ and (b) F^+ ions underwent double-electron-capture reactions with $CHCl_3$ molecules.

states, so that several additional peaks in the DCT spectra of these molecules have here been observed and analysed.

Acknowledgements

One of the authors (R.P.G.) thanks the University of Wales for the award of a postgraduate studentship. They thank the British Mass Spectrometry Society for a grant that allowed the GAUSSIAN program to be purchased.

References

[1] E. Wigner, Nachr. Akad. Wiss. Goettingen, Math. Phys. IIa (1927) 325.
[2] F.M. Harris, Int. J. Mass Spectrom. Ion Processes 120 (1992) 1.
[3] W.J. Griffiths, F.M. Harris, Rapid Commun. Mass Spectrom. 2 (1988) 28.
[4] W.J. Griffiths, F.M. Harris, Rapid Commun. Mass Spectrom. 2 (1988) 91.
[5] S.R. Andrews, F.M. Harris, Rapid Commun. Mass Spectrom. 7 (1993) 548.
[6] R.P. Grant, F.M. Harris, S.R. Andrews, D.E. Parry, Int. J. Mass Spectrom. Ion Processes 142 (1995) 117.
[7] S.R. Andrews, D.E. Parry, Chem. Phys. Lett. 196 (1992) 630.
[8] J.C. Slater, K.H. Johnson, Phys. Rev. B 5 (1972) 844.
[9] J. Schirmer, A. Barth, Z. Phys. A 317 (1984) 267.
[10] F. Tarantelli, A. Tarantelli, A. Sgamellotti, J. Schirmer, L.S. Cederbaum, Chem. Phys. Lett. 117 (1985) 577.
[11] F. Tarantelli, A. Sgamellotti, L.S. Cederbaum, J. Schirmer, J. Chem. Phys. 86 (1987) 2201.
[12] E.M.-L. Ohrendorf, F. Tarantelli, L.S. Cederbaum, J. Chem. Phys. 92 (1990) 2984.
[13] D. Minelli, F. Tarantelli, A. Sgamellotti, L.S. Cederbaum, J. Electron Spectrosc. Relat. Phenom. 10 (1996) 1693.
[14] D.E. Parry, Int. J. Quantum Chem. 64 (1997) 175.
[15] A.B. Trofimov, J. Schirmer, J. Phys. B 28 (1995) 2299.
[16] D.E. Parry, Prog. Theoret. Chem. Phys., in press.
[17] I.W. Griffiths, D.E. Parry, F.M. Harris, Int. J. Mass Spectrom. 185/186/187 (1999) 651.
[18] M.J. Frisch, G.W. Trucks, H.B. Schegel, P.M.W. Gill, B.G. Johnson, M.A. Robb, J.R. Cheeseman, T. Keith, G.A. Peterson, J.A. Montgomery, K. Raghavachari, M.A. Al-Laham, V.G. Zakrzewski, J.V. Ortiz, J.B. Foresman, J. Cioslowski, B.B. Stefanov, A. Nanayakkara, M. Challacombe, C.Y. Peng, P.Y. Ayala, W. Chen, M.W. Wong, J.L. Andres, E.S. Replogle, R. Gomperts, R.L. Martin, D.J. Fox, J.S. Binkley, D.J. Defrees, J. Baker, J.J.P. Stewart, M. Head-Gordon, C. Gonzalez, J.A. Pople, GAUSSIAN94, Revision E.1, Gaussian Inc., Pittsburg PA, 1995.
[19] C.C. Costain, J. Chem. Phys. 29 (1958) 864.
[20] R.J. Myers, W.D. Gwinn, J. Chem. Phys. 20 (1952) 1420.
[21] P.N. Wolfe, J. Chem. Phys. 25 (1956) 976.
[22] N. Jeffreys, S.R. Andrews, D.E. Parry, F.M. Harris, Rapid Commun. Mass Spectrom. 10 (1996) 1693.
[23] C.E. Moore, Atomic Energy Levels, National Bureau of Standards, Gaithersburg, MD, 1949.
[24] P. Fournier, C. Benoit, J. Durup, R.E. March, C.R. Acad. Sci. Paris Ser. B 278 (1974) 1039.
[25] D. Mathur, Int. J. Mass Spectrom. Ion Processes 83 (1988) 203.
[26] D.P. Almeida, M.L. Langford, Int. J. Mass Spectrom. Ion Processes 96 (1990) 331.
[27] M.L. Langford, F.M. Harris, Rapid Commun. Mass Spectrom. 4 (1990) 125.